

## Level structure of $^{89}\text{Mo}$

G. García-Bermúdez,\* M. A. Cardona, R. V. Ribas,† A. Filevich, E. Achterberg, and L. Szybisz\*  
*Laboratorio TANDAR, Departamento de Física, Comisión Nacional de Energía Atómica, Av. del Libertador 8250,  
 1429 Buenos Aires, Argentina*

(Received 17 September 1992; revised manuscript received 11 June 1993)

The level structure of  $^{89}\text{Mo}$  has been studied with the  $^{60}\text{Ni}(^{32}\text{S},2pn)$  reaction at 110 MeV beam energy. Mainly two bands of  $\gamma$  rays depopulating states of probable spin-parity values ranging up to  $(27/2)^+$  were determined from the excitation function, neutron and  $\gamma$ - $\gamma$  coincidences, and  $\gamma$ -ray angular distributions. The high-spin states of  $^{89}\text{Mo}$  show a scheme very similar to that of the  $^{87}\text{Zr}$  isotope. The interpretation of these states in terms of the three neutron-hole configuration  $(\nu g_{9/2})^{-3}$  and core-excited states is discussed.

PACS number(s): 27.50.+e

### I. INTRODUCTION

The purpose of this investigation is to establish the decay scheme of  $^{89}\text{Mo}$ . This nucleus, which lies in the vicinity of the closed  $N = 50$  shell, is expected to present features of spherical nuclei with three neutron-hole excitations.

Let us now outline the scarce information available on the decay scheme of the excited states of  $^{89}\text{Mo}$  [1]. This nucleus was investigated for the first time by Pardo *et al.* [2] with the  $^{92}\text{Mo}(^3\text{He},^6\text{He})$  reaction. They proposed a few low-energy levels, in particular, a low-lying  $I^\pi = (7/2^+)$  state at an excitation energy of 124 keV and a  $(1/2^-)$  isomeric level at about 400 keV. This isomer as well as other levels has also been analyzed by de Boer *et al.* [3] with the  $^{90}\text{Zr}(^3\text{He},4n)$  reaction. On the basis of their findings these authors reported a preliminary level scheme for  $^{89}\text{Mo}$ . In addition, the decay properties of the  $(1/2^-)$  isomeric level have been studied by Gallagher *et al.* [4] in an experiment where a  $^{92}\text{Mo}$  target was irradiated by a 60 MeV proton beam. They established that the isomer lies at 387.3 keV and decays with a half-life of  $190 \pm 15$  ms.

In summary, due to the light-ion beam used in all previous investigations it was only possible to determine the existence of few low-lying levels with small spin. Furthermore, the proposed spin-parity assignment relied mainly on systematic trends of low-lying states of the adjacent  $N = 47$  isotones  $^{87}\text{Zr}$  and  $^{85}\text{Sr}$ . Thus, in order to increase the information about  $^{89}\text{Mo}$ , it has been the purpose of the present work to measure the high-spin decay scheme of this nucleus via a reaction induced by a heavier projectile, as  $^{32}\text{S}$ . The paper is organized as follows. The experimental setup as well as the procedures employed

for the measurements are reported in Sec. II. A description of the isotopic identification is presented in Sec. III. The level scheme is given in Sec. IV. Finally, Sec. V is devoted to a discussion and conclusions.

### II. EXPERIMENTAL PROCEDURE AND RESULTS

The high-spin states of  $^{89}\text{Mo}$  were populated by the reaction  $^{60}\text{Ni}(^{32}\text{S},2pn)$  produced at the Buenos Aires TANDAR accelerator. The target consisted of a  $1.5 \text{ mg/cm}^2$  foil of  $^{60}\text{Ni}$  enriched to 99.9%, which was backed with an  $8 \text{ mg/cm}^2$  foil of natural lead in order to stop the recoiling nuclei. Gamma-ray singles spectra were measured with a Compton suppressed HPGe detector of 30% efficiency at several beam energies, ranging from 110 up to 140 MeV in 10 MeV steps. The evaporation code PACE4 predicts at about 110 MeV a strong population of the  $2pn$  channel, which leads to  $^{89}\text{Mo}$ . Figure 1 shows a  $\gamma$ -ray singles spectrum in which the other important reaction channels were identified as  $3p$ ,  $\alpha 2p$ ,  $4p$ , and  $3pn$  leading to  $^{89}\text{Nb}$ ,  $^{86}\text{Zr}$ ,  $^{88}\text{Zr}$ , and  $^{88}\text{Nb}$ , respectively.

Further identification was accomplished by analyzing neutron- $\gamma$  coincidence spectra measured at the same beam energies as those used for the excitation functions. The neutrons were detected with a 127 mm diameter by 127 mm long cylinder filled with NE213 liquid scintillator. This detector was positioned at 10 cm from the target and at  $0^\circ$  relative to the beam direction and to decrease the number of detected  $\gamma$  rays it was covered with a 4 cm thick lead shield. The standard pulse shape discrimination technique was used to separate neutrons from  $\gamma$  rays. A HPGe detector of 40% efficiency located at  $135^\circ$  measured the  $\gamma$ -ray spectrum in coincidence with the neutron signal. The data obtained at 110 MeV are shown in Fig. 2.

The  $\gamma$ -ray angular distributions were measured using a standard procedure with a cylindrical chamber and two detectors placed at a distance of 12 cm from the target. One of them, a Compton suppressed HPGe detector, was rotated to measure  $\gamma$ -ray spectra at seven angles ( $0^\circ$ ,  $15^\circ$ ,

\*Also at the Carrera del Investigador Científico of the Consejo Nacional de Investigaciones Científicas y Técnicas, Argentina.

†Present address: Instituto de Física, Universidade de São Paulo, BR-01498 São Paulo, Brazil.

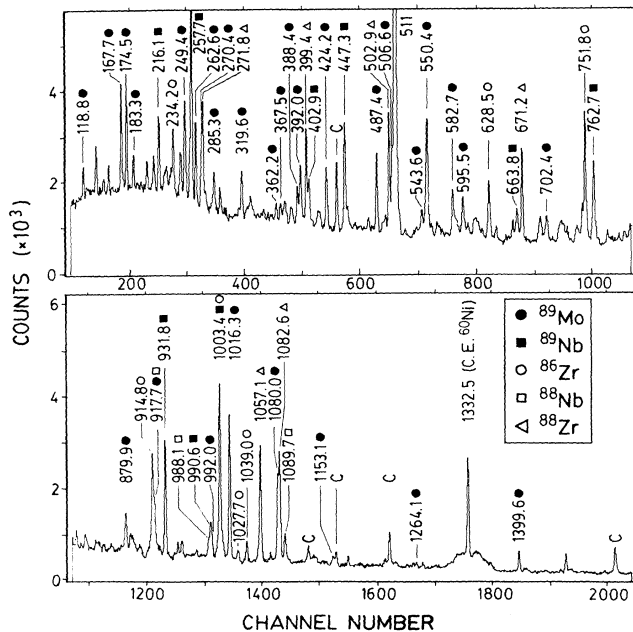


FIG. 1. Single Compton suppressed  $\gamma$ -ray spectrum from the  $^{60}\text{Ni}(^{32}\text{S},X)$  reaction at 110 MeV beam energy. Several reaction channels are labeled. The letter *C* stands for background unidentified  $\gamma$  rays.

$30^\circ$ ,  $45^\circ$ ,  $60^\circ$ ,  $75^\circ$ , and  $90^\circ$ ) with respect to the beam direction. The other one (a 30% efficiency HPGe detector) was held at  $135^\circ$  and used to determine  $\gamma$ -ray intensities in order to normalize the different spectra. The results for the singles intensities as well as the corresponding angular distribution coefficients  $A_{22}$  and  $A_{44}$  are listed in Table I.

For the  $\gamma$ - $\gamma$  coincidence experiment we used a Compton suppressed HPGe detector of 30% efficiency placed at  $0^\circ$  with respect to the beam direction in coincidence with a HPGe detector of 40% efficiency positioned at  $135^\circ$ . The measurements were performed at 110 MeV beam energy and from their analysis two groups of  $\gamma$  rays were determined. Some examples of gated spectra are plotted in Fig. 3.

A preliminary level scheme obtained from the experiments described above has already been published elsewhere [5]. The revised and completed final version is shown in Fig. 4.

### III. ISOTOPIC IDENTIFICATION

As described in the preceding section, two different sorts of experiments, namely excitation function and neutron- $\gamma$  coincidence, were performed in order to obtain

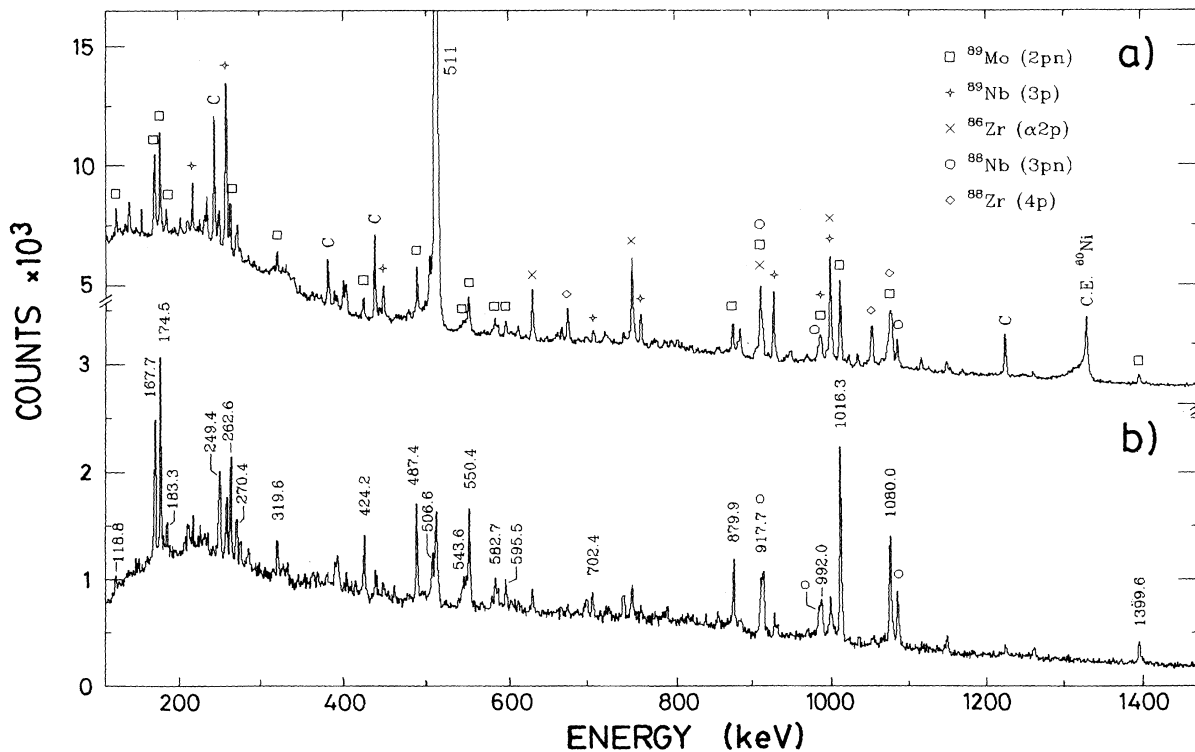


FIG. 2. (a) A  $\gamma$ -ray single spectrum from the  $^{60}\text{Ni}(^{32}\text{S},X)$  at 110 MeV energy in which several reaction channels are indicated. The letter *C* stands for unidentified  $\gamma$  rays. (b) The neutron- $\gamma$  coincidence spectrum in which most of intense transitions, labeled by the energy, are from the decay of  $^{89}\text{Mo}$ . A few transitions from the neutron channel leading to  $^{88}\text{Nb}$  are also indicated.

TABLE I. Energies, intensities, and angular distribution coefficients of  $\gamma$  rays assigned to  $^{89}\text{Mo}$ . The error in the last digit is given in parentheses.

$E_\gamma$	$I_\gamma$	$A_{22}$	$A_{44}$	$E_\gamma$	$I_\gamma$	$A_{22}$	$A_{44}$
118.8(3)	5(1)			550.5(3)	7 <sup>a</sup>		
167.7(2)	18(4)	0.22(5)	-0.14(10)	582.7(2)	15(2)	-0.53(6)	0.14(10)
174.5(2)	21(3)	0.37(6)	-0.06(6)	595.5(2)	17(3)		
183.3(2)	4 <sup>a</sup>			696.5(3)	3 <sup>a</sup>		
249.4(3)	17(3)	-0.58(6)	0.03(12)	702.4(2)	10(2)		
262.6(2)	17(3)	0.13(6)	-0.06(6)	845.3(4)	3 <sup>a</sup>		
268.8(3)	4(1)			879.9(2)	27(4)	0.11(6)	0.08(8)
319.6(2)	9(1)			917.7(3)	19(3)		
362.2(4)	6(1)			992.0(3)	17(3)		
367.5(4)	3(1)			1016.3(2)	100(12)	0.28(6)	-0.08(6)
424.2(2)	14(2)	-0.60(10)	0.19(10)	1080.0(2)	60(8)	0.26(6)	-0.06(2)
487.4(2)	27(4)	0.15(6)	-0.03(3)	1102.1(3)	3 <sup>a</sup>		
506.6(3)	23(4)			1399.6(4)	16(2)	0.25(8)	-0.10(7)
543.6(3)	6(1)			1526.9(4)	weak		
550.4(2)	34(5)	-0.54(6)	0.14(8)	1646.1(4)	weak		

<sup>a</sup>Estimated from coincidence results, the corresponding errors are about 30%.

the isotopic identification of the measured  $\gamma$  rays. Several transitions observed in the excitation measurement were identified and ascribed to the decay of known nuclei as shown in Fig. 1. The scarce knowledge about  $^{89}\text{Mo}$  obtained from previous works [2,3] made the identification difficult of the  $\gamma$  rays belonging to this nucleus.

Most of the numerous  $\gamma$  rays found in this study can be collected into two groups with different intensities as a function of beam energy. One of them, with a maximum intensity at about 110 MeV, corresponds to three-particle evaporation residues. At this energy there are several, not previously identified, strong  $\gamma$ -rays exhibiting excita-

tion functions similar to those of known three-particle channels. These transitions, for instance, the 167.7, 174.5, 550.4, 879.9, 1016.3 keV lines, are greatly enhanced in the neutron- $\gamma$  spectrum as indicated in Fig. 2. More information was obtained from a PACE4 evaluation by looking at results yielded for reactions involving the evaporation of three particles, one of them being a neutron. According to such a calculation, the cross section for the  $2pn$  channel at 110 MeV is one order of magnitude larger than that for the competing  $\alpha pn$  channel. Further evidence was provided by the  $\gamma$ - $\gamma$  coincidence experiment. From all the above-mentioned arguments,

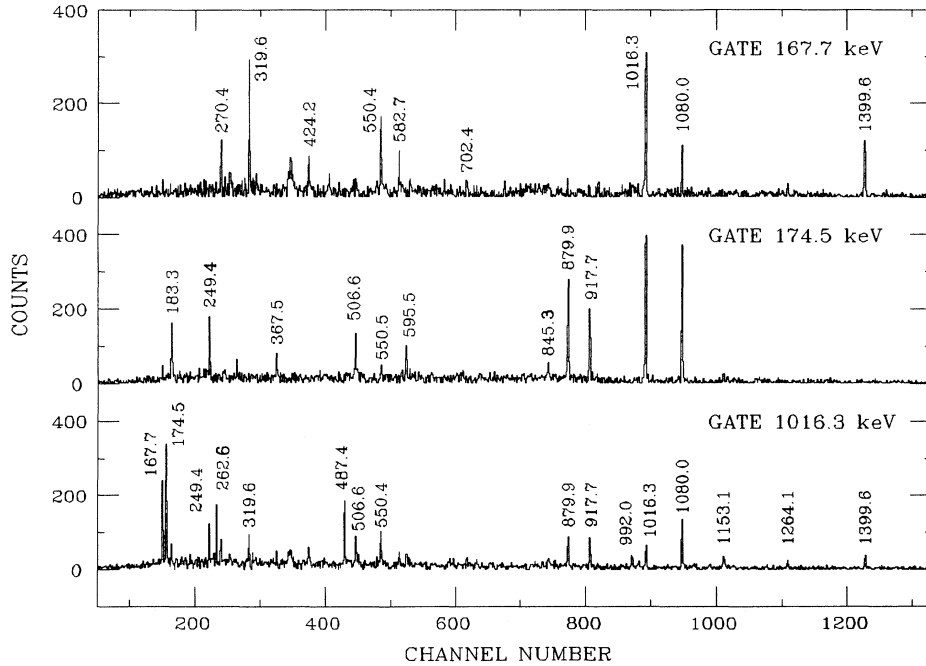


FIG. 3. The  $\gamma$ - $\gamma$  coincidence spectra obtained by gating on the 167.7, 174.5, and 1016.3 keV  $\gamma$  rays.



1526.9 and 1646.1 keV transitions, respectively. This fact suggests an  $(11/2^+)$  assignment for it.

The decay scheme above the 2096.3 keV level is separated into two independent  $\gamma$ -ray cascades. This observation suggests that these cascades deexcite levels of different parity. The one of probable positive parity was just described in the preceding subsections. The other cascade strongly populates the 2270.9 keV state, which in turn is deexcited through the 174.5 and 262.6 keV  $\gamma$  rays. The positive values of the  $A_{22}$  coefficients quoted in Table I might suggest a common quadrupole character for both transitions, but such a description cannot account for their similar intensities and one must perform a more elaborate analysis. On the basis of experimental data one is practically forced to assign a  $\Delta I = 2$  character to the 262.6 keV  $\gamma$  ray. However, the particularly large positive value of  $A_{22} = 0.37(6)$  for the 174.5 keV  $\gamma$  ray makes it possible to interpret it as a  $\Delta I = 0$  transition [7]. The similarity of the observed intensities can be well understood, since a 174.5 keV dipole transition involving a change of parity (e.g., a  $10^4$  hindered  $E1$  decay) may compete successfully with a quadrupole transition of 262.6 keV. Therefore, we suggest an isomeric  $I^\pi = (17/2^-)$  state at 2270.9 keV and a  $(13/2^-)$  state at 2000.8 keV. Further support to our assignment is given by the fact that the decay of this 2270.9 keV level is similar to that of the isomeric  $17/2^-$  state of 2.7 ns at 2314 keV in  $^{87}\text{Zr}$  (see Ref. [9]).

Towards higher-energy levels the weak intensity and the lack of angular distribution results make the assignment procedure very difficult. Concluding, there were several  $\gamma$  rays, assigned to the decay of  $^{89}\text{Mo}$ , not placed in the present decay scheme. For instance, the coincidence spectrum gated in the 1016.3 keV  $\gamma$  ray (see Fig. 3) presents a  $\gamma$  ray at the same energy, namely 1016.3 keV. From an intensity measurement in the spectra gated by the 1016.3, 879.9, and 1080.1 keV lines it was possible to determine that the intensity of the unplaced  $\gamma$  ray is about 10% of the known one decaying to the ground state. Furthermore, the coincidence data give evidence that the missing  $\gamma$  ray feeds the cascade which finally feeds the 2270.9 keV level.

Other transitions seen in coincidence with the strong 1016.3 keV line, which were not placed in the decay scheme are the 270.4, 285.3, 388.4, 392.0, 1153.1, and 1264.1 keV  $\gamma$  rays.

## V. DISCUSSION AND CONCLUSIONS

We shall now discuss the level structure of  $^{89}\text{Mo}$  ( $Z = 42$  and  $N = 47$ ). Since this nucleus has only three neutron holes in the closed  $N = 50$  shell, one could expect that it would mainly present properties of spherical nuclei. In order to provide more arguments in favor of such an assumption and to get a correct interpretation of our results for  $^{89}\text{Mo}$ , it is useful to review the available information in this mass region. For instance, an important guide for the understanding of the level scheme reported in Fig. 4 is the analysis of the properties of the chain of zirconium ( $Z = 40$ ) isotopes. A very large se-

ries of these isotopes (from  $N = 40$  up to  $N = 64$ ) has been carefully investigated and data show an interesting interplay of collective and single-particle degrees of freedom. Thus, at neutron numbers  $N = 40$  and 64, zirconium exhibits a strong collectivity with quadrupole deformations of  $\beta_2 \sim 0.4$  [10,11], while around  $N = 50$  the spherical neutron shell closure dominates and no evidence for collectivity was found [9,12–16]. Moreover, the changes occur rather suddenly at  $N = 45$  and 55; for  $46 \leq N \leq 54$  there are almost no collective band structures and the quadrupole matrix elements do not show an important collective enhancement. Very similar features have also been seen in the chain of strontium ( $Z = 38$ ) isotopes, which indicates that properties described above are not much disturbed by the different number of protons. This has been the situation until a couple of years ago and in such a scenario one could infer that the chain of molybdenum isotopes might present similar characteristics. We have undertaken the study of  $^{89}\text{Mo}$  in order to seek whether this analogy indeed holds [5]. Simultaneously with our research this conjecture has also been thoroughly investigated in the cases of  $^{87}\text{Mo}$  by Winter *et al.* [17], of  $^{88}\text{Mo}$  by Weiszflog *et al.* [18], and of  $^{90}\text{Mo}$  by Kabadiyski *et al.* [19]. These authors found that  $^{87}\text{Mo}$  ( $N = 45$ ) is a transitional nucleus exhibiting both collective and noncollective features, while  $^{88}\text{Mo}$  ( $N = 46$ ) and  $^{90}\text{Mo}$  ( $N = 48$ ) can be described by a shell model approach. Hence, nowadays it is reasonable to suppose that  $^{89}\text{Mo}$  should also exhibit a near-spherical behavior. Since a shell model calculation goes beyond the scope of this experimental work, we shall interpret the structure of this nucleus on the basis of a systematic comparison with known neighbors. Of course, while this procedure can only provide schematic results, interesting conclusions may nevertheless be drawn.

Let us first pay attention to positive-parity states. Looking at Fig. 4 one notices that the  $^{60}\text{Ni}(^{32}\text{S},2pn)$  reaction strongly populates the cascade connecting the yrast levels 2584 keV ( $21/2^+$ ), 2096 keV ( $17/2^+$ ), and 1016 keV ( $13/2^+$ ) to the  $9/2^+$  ground state. In what follows of the discussion we shall suppress the parenthesis of the spins. Similar cascades have already been observed in the neighboring  $N = 47$  isotones  $^{85}\text{Sr}$  [20,21] and  $^{87}\text{Zr}$  [9]. In the literature [9,14] it is suggested that the low-lying states of these  $\gamma$ -ray cascades can be associated with the coupling of a neutron hole  $(\nu g_{9/2})^{-1}$  to the  $I^\pi = 0^+, 2^+, \text{ and } 4^+$  core excitations of the  $(Z, N + 1)$  adjacent even-even nuclei. Figure 5 shows a comparison between the energy of low-lying positive-parity yrast levels of the  $N = 47$  isotones and those of the  $^{86}\text{Sr}$ ,  $^{88}\text{Zr}$ , and  $^{90}\text{Mo}$   $N = 48$  isotones. From this figure it becomes evident that there are common features in the structure of low-lying states of all these nuclei. This odd-even parallelism has been found in many transitional nuclei. The doubly even nuclei shown in Fig. 5 exhibit a very similar structure up to the  $8_1^+$  yrast level, which is an isomer with half-life  $T_{1/2} = 0.46 \mu\text{s}$  in  $^{86}\text{Sr}$ ,  $T_{1/2} = 1.75 \mu\text{s}$  in  $^{88}\text{Zr}$ , and  $T_{1/2} = 1.05 \mu\text{s}$  in  $^{90}\text{Mo}$ . One would naively expect all the  $I^\pi = 0^+, 2^+, 4^+, 6^+, \text{ and } 8_1^+$  yrast states to consist primarily of some mixture of the  $(\nu g_{9/2})_I^{-2}$  and  $(\pi g_{9/2})_I^2$  excitations. However, the location of the very

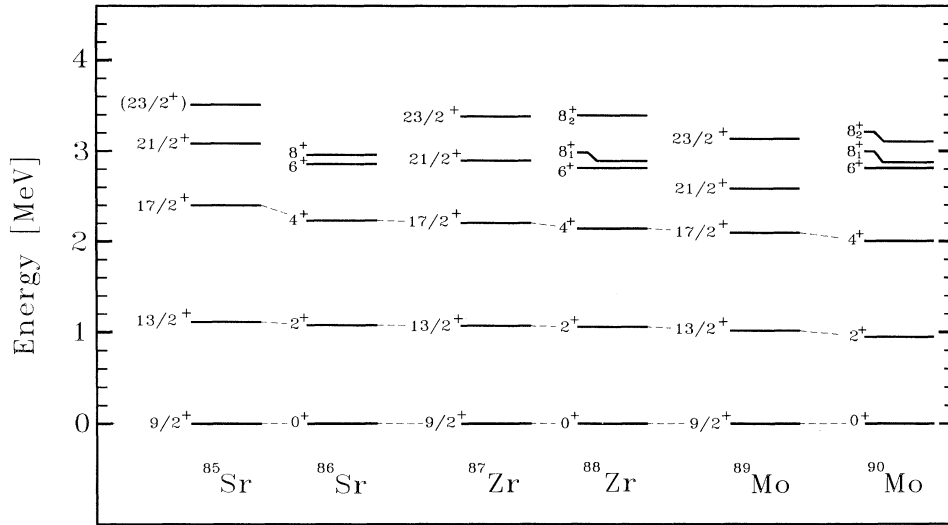


FIG. 5. Comparison of low-lying positive-parity levels for the  $N = 47$  odd-even isotones  $^{85}\text{Sr}$ ,  $^{87}\text{Zr}$ , and  $^{89}\text{Mo}$  and those for the  $N = 48$  even-even isotones  $^{86}\text{Sr}$ ,  $^{88}\text{Zr}$ , and  $^{90}\text{Mo}$ .

closely placed  $6^+$  and  $8_1^+$  levels, being almost independent of  $Z$ , suggests for these states a wave function dominated by neutron configurations. In fact, the measured  $g$  factor of the  $8_1^+$  state in  $^{86}\text{Sr}$  [22], i.e.,  $g = -0.243$ , coincides with the experimental value [23] obtained for the  $g$  factor of the  $9/2^+$  ground state of the  $N = 49$   $^{87}\text{Sr}$ , indicating a pure neutron aligned  $(\nu g_{9/2})_{I=8}^{-2}$  configuration for this isomeric state. In addition, the measurements [24] of the  $g$  factor in the cases of  $^{88}\text{Zr}$  ( $g = -0.227$ ) and  $^{90}\text{Mo}$  ( $g = -0.174$ ) indicate that the structure of the  $8_1^+$  state of these heavier nuclei may be interpreted in terms of a dominating neutron alignment with a small proton admixture which increases for increasing  $Z$ . Furthermore, according to calculations of de Boer *et al.* [25] and Oxorn *et al.* [26], the lower-spin  $I^+$  yrast states also contain a strong neutron component  $(\nu g_{9/2})_I^{-2}$  with an admixture of the proton  $(\pi g_{9/2})_I^2$  configuration.

Figure 5 shows that the energies of the  $13/2^+$  and  $17/2^+$  levels agree rather well with those of the  $I^\pi = 2^+$  and  $4^+$  states of adjacent doubly even nuclei; nevertheless, note a slight but systematic compression with increasing mass number  $A$ . On the basis of its location, these low-lying states can be mainly attributed to the coupling of a hole  $(\nu g_{9/2})^{-1}$  to the core excitations described above. This scheme gives rise to seniority-three excitations of the type  $(\nu g_{9/2})^{-3}$  and  $(\nu g_{9/2})^{-1}(\pi g_{9/2})_I^2$ . Taking into account that the energy of the  $17/2^+$  level varies as a function of  $Z$  more pronouncedly than that of the  $13/2^+$  level, one could suggest that the contribution of the  $(\nu g_{9/2})^{-1}(\pi g_{9/2})_I^2$  configuration should be more important in the former case.

On the other hand, the comparison of energies of the  $21/2^+$  levels with those of the  $6^+$  states does not show the regular behavior of the lower-lying ones. This fact is an indication that the  $21/2^+$  states have a more complex structure than the other members of these  $I \rightarrow I - 2$  yrast cascades. Probably, besides the expected  $(\nu g_{9/2})^{-3}$  and  $(\nu g_{9/2})^{-1}(\pi g_{9/2})_{I=6}^2$  contributions,

there is an important admixture of the configuration  $(\nu g_{9/2})^{-1}(\pi g_{9/2})_{I=8}^2$  as well as of higher-seniority excitations like  $(\nu g_{9/2})_{I_n}^{-3}(\pi g_{9/2})_{I_p}^2$ . It should be pointed out that  $21/2^+$  is the highest spin allowed by the seniority-three  $(\nu g_{9/2})^{-3}$  multiplet.

Figure 4 shows that the  $21/2^+$  state is strongly fed by an  $M1$  transition from the  $23/2^+$  level. This feature has also been observed in  $^{87}\text{Zr}$  (cf. Fig. 5 in [9]). Both  $23/2^+$  levels have been included in Fig. 5, where one realizes that they lie at almost the same energy as the  $8_2^+$  levels of adjacent  $(Z, N + 1)$  nuclei. The  $8_2^+$  states in even-even neighbors are dominated by the proton aligned  $(\pi g_{9/2})_{I=8}^2$  configuration (see discussions in Refs. [25,26]). Therefore it is reasonable to assume that these  $23/2^+$  levels are mainly  $(\nu g_{9/2})^{-1}(\pi g_{9/2})_{I=8}^2$  states with a weaker contribution of seniority-five  $(\nu g_{9/2})_{I_n}^{-3}(\pi g_{9/2})_{I_p}^2$  configurations. This kind of wave function favors the high rate of the  $23/2^+ \rightarrow 21/2^+$   $M1$  transition and, therefore, strongly supports the proton admixtures suggested above for the  $21/2^+$  yrast state. Although a  $23/2^+$  level has also been determined at a comparable energy in  $^{85}\text{Sr}$  (see Fig. 5), its structure must be different because it does not deexcite via the  $21/2^+$  yrast state (cf. Fig. 2 in [21]). Furthermore, it cannot be associated with a close-energy proton aligned  $8_2^+$  state in  $^{86}\text{Sr}$ , since no evidence has yet been found for such a level [27].

The similarities between the level schemes of  $^{87}\text{Zr}$  and  $^{89}\text{Mo}$  displayed in Fig. 5 can be extended further. Figure 6 shows our results for the positive-parity states in  $^{89}\text{Mo}$  compared with those of  $^{87}\text{Zr}$  measured by Arnell *et al.* [9]. On top of the  $23/2^+$  levels there are located three more states with spins  $25/2_1^+$ ,  $25/2_2^+$ , and  $27/2^+$ . Both  $25/2^+$  states may be interpreted in terms of the same configurations ascribed to the  $23/2^+$  one, the differences being due to changes in the coupling of the neutron-hole clusters  $(\nu g_{9/2})_{I_n}^{-3}$  to the aligned protons. Since the seniority-three  $(\nu g_{9/2})^{-1}(\pi g_{9/2})_{I=8}^2$  multiplet

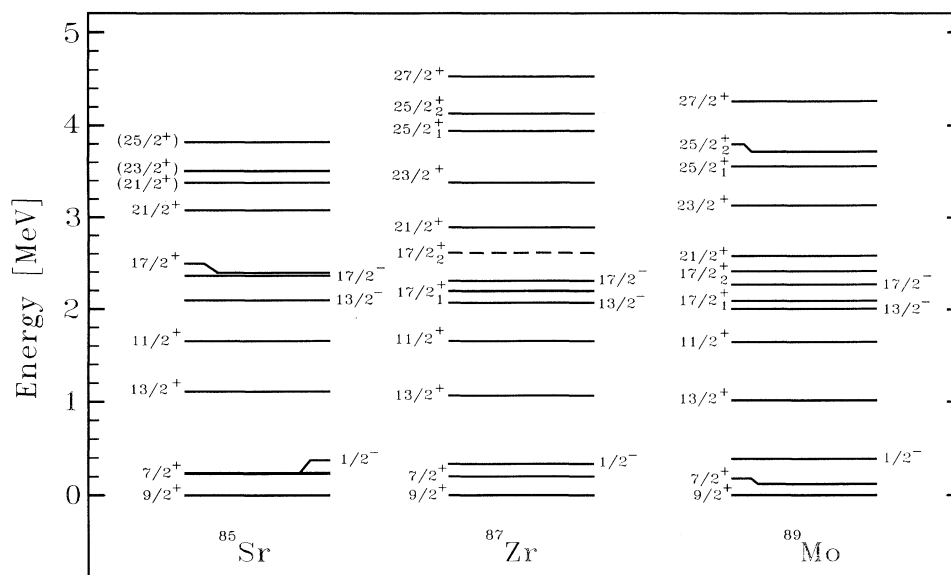


FIG. 6. Comparison between the most populated levels in  $^{89}\text{Mo}$  and their counterparts in the  $N = 47$  odd-even isotones  $^{85}\text{Sr}$  and  $^{87}\text{Zr}$ .

only reaches up to spin  $25/2^+$ , the  $27/2^+$  state should be described by at least seniority-five configurations of type  $(\nu g_{9/2})^{-3}(\pi g_{9/2})^2_{I=8}$ . There is no crossover transition found within these  $27/2^+ \rightarrow 25/2^+ \rightarrow 23/2^+ \rightarrow 21/2^+$  cascades because  $E2$  transitions cannot compete with the fast  $M1$  transitions. On the other hand, it is remarkable that a fast  $25/2^+ \rightarrow 23/2^+ \rightarrow 21/2^+$   $M1$  cascade has also been observed at similar energies in  $^{91}\text{Mo}$  ( $Z = 42, N = 49$ ), where the nuclear structure is clearly dominated by the  $(\nu g_{9/2})^{-1}(\pi g_{9/2})^2_I$  configuration [28].

Furthermore, Kemnitz *et al.* [29] studied the  $^{83}\text{Kr}$  nucleus, isotone of  $^{89}\text{Mo}$ , establishing a  $\Delta I = 1$   $\gamma$ -ray cascade from  $21/2^+$  up to  $29/2^+$ , which was interpreted as a  $(\nu g_{9/2})(\pi g_{9/2})^2$  configuration. The observation of strong  $M1$   $\gamma$  rays depopulating these levels in several nuclei of this mass region supports to such an interpretation, see Refs. [29,30]. Dönau *et al.* [31], using a semiclassical relation, explain this  $M1$  enhancement as a result of a particular three-quasiparticle (3qp) configuration consisting of a strongly coupled neutron and two almost aligned protons. The result of a search for similar 3qp configurations in the 80–90 mass region is shown in Fig. 7, where the levels are normalized to the energy of the  $23/2^+$  state. The similarities exhibited by this drawing for the isotonic chain  $N = 43, 45$ , and  $47$  suggest the assignment of a common nuclear structure to all these levels.

On the other hand, we determined a second  $17/2^+$  state, which is equivalent to that tentatively suggested by Arnell *et al.* [9] for  $^{87}\text{Zr}$ . The low-lying  $7/2^+$  state present in both nuclei and shown in Fig. 6 is an important feature of the seniority-three neutron  $(\nu g_{9/2})^{-3}_I$  configuration (see discussion of Kitching *et al.* [14]). In addition, this seniority-three neutron excitation also explains the location of  $11/2^+$  states displayed in the same figure. It is worthwhile to note that the  $7/2^+$  and  $11/2^+$  states have been also found [20,21] at almost the same energies

in  $^{85}\text{Sr}$ . Therefore, in order to facilitate a direct comparison we include in Fig. 6 also a basic level scheme of this nucleus.

Our new information on negative-parity states is rather poor. Due to the lack of data on  $\gamma$ -ray angular distributions, the identification of the probable negative-parity high-spin states above the 2279 keV ( $17/2^-$ ) level was not possible. Only the  $13/2^-$  and  $17/2^-$  states could be identified unambiguously. Both these levels have counterparts in the level schemes of  $^{85}\text{Sr}$  and  $^{87}\text{Zr}$  as shown in Fig. 6. In the cases of  $^{87}\text{Zr}$  and  $^{89}\text{Mo}$  the  $17/2^-$  level decays to the  $17/2^+$  yrast and the negative-parity  $13/2^-$  state emitting two low-energy  $\gamma$  rays, whereas in  $^{85}\text{Sr}$  the  $17/2^-$  level lies below the  $17/2^+$  yrast state and therefore decays to the  $13/2^-$  state. In turn, the latter level always decays primarily to the  $11/2^+$  and  $13/2^+$  yrast states. These negative-parity states may be interpreted as a coupling of the neutron hole  $(\nu g_{9/2})^{-1}$  to the  $I^\pi = 4^-$  and  $5^-$  yrast core excitations of the adjacent ( $Z, N + 1$ ) nuclei. These core excitations are mainly seniority-two proton particles or neutron holes in the  $p_{1/2}$  and  $g_{9/2}$  configurations. In the case of  $^{88}\text{Zr}$  the calculations of Refs. [25,26]

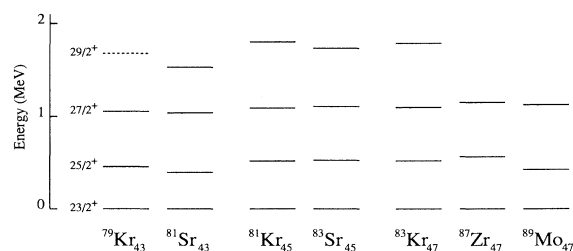


FIG. 7. Systematic of states interpreted as a  $(\nu g_{9/2})(\pi g_{9/2})^2$  three-quasiparticle (3qp) configuration for odd Kr, Sr, Zr, and Mo isotopes. The energies are normalized to that of the  $23/2^+$  level.

both indicate that the  $5^-$  yrast state is dominated by the  $[(\pi g_{9/2})(\pi p_{1/2})]_5$  configuration, whereas for  $^{90}\text{Mo}$  the theoretical results differ. The calculation of de Boer *et al.* [25] yielded a mixed wave function with a dominance of the neutron-hole  $[(\nu g_{9/2})^{-1}(\nu p_{1/2})^{-1}]_5$  configuration, while Oxorn *et al.* [26] obtained that the proton configuration is the most important one as in  $^{88}\text{Zr}$ . Therefore on the basis of these calculations no meaningful guess can be made about the structure of the  $13/2^-$  and  $17/2^-$  yrast states in  $^{89}\text{Mo}$ . In spite of this fact, it is interesting to point out that Fig. 6 indicates that the location of these states is almost independent of  $Z$ , resembling the behavior of the neutron aligned  $6^+$  and  $8_1^+$  states in adjacent even-even nuclei.

Finally, the low-lying  $1/2^-$  state present in all the  $N = 47$  isotones shown in Fig. 6 is interpreted [9,14] as a single neutron hole  $(\nu p_{1/2})^{-1}$  coupled to the ground state of the even-even core.

In conclusion, the present determination of the previously unknown decay scheme of  $^{89}\text{Mo}$  results in a very similar structure compared to the isotope  $^{87}\text{Zr}$ . Thus the  $^{87}\text{Zr}$ - $^{89}\text{Mo}$  pair of nuclei strikingly exhibits an almost identical energy pattern, although a slight compression

for positive-parity high-spin states in  $^{89}\text{Mo}$  is apparent. Certainly, more experimental work, in particular lifetime measurements, is needed to reduce the uncertainty in the configuration assignment.

*Note added.* We have learned of results of S. Wen *et al.* reported in *Proceedings of the 1992 International Nuclear Physics Conference*, Wiesbaden, Germany, edited by Organizing Committee, Book of Abstracts, contribution 1.2.10. Their results are in agreement with those presented here. Furthermore, a work by Weiszflog *et al.* has recently been published in *Z. Phys. A* **344**, 395 (1993); their results agree with ours and add several new levels at higher angular momenta.

#### ACKNOWLEDGMENTS

The authors acknowledge partial support from the PID-CONICET and from the Fundación Antorchas. One of the authors (R.V.R.) thanks the financial support received from the Argentina-ICTP Scientific Cooperation Programme.

- [1] H. Sievers, *Nucl. Data Sheets* **58**, 351 (1989).
- [2] R. C. Pardo, L. W. Robinson, W. Benenson, E. Kashy, and R. M. Ronningen, *Bull. Am. Phys. Soc.* **24**, 648 (1979); *Phys. Rev. C* **21**, 462 (1980).
- [3] F. W. N. de Boer, C. A. Fields, R. A. Ristinen, L. E. Samuelson, and P. A. Smith, University of Colorado Cyclotron Report COO-535-767, 1979 (unpublished), p. 89.
- [4] P. W. Gallagher, E. W. Schneider, and W. B. Walter, *Z. Phys. A* **296**, 81 (1980).
- [5] G. García-Bermúdez, R. V. Ribas, M. A. Cardona, A. Filevich, E. Achterberg, and L. Szybisz, in *Proceedings of the 1989 International Nuclear Physics Conference*, São Paulo, Brasil, edited by Organizing Committee (University of São Paulo, São Paulo, 1989), Vol. 1, p. 207.
- [6] P. W. Gallagher, N. K. Aras, and W. B. Walters, *Phys. Rev. C* **23**, 873 (1981).
- [7] E. Der Mateosian and A. W. Sunyar, *At. Data Nucl. Data Tables* **13**, 407 (1974).
- [8] P. Taras and B. Hass, *Nucl. Instrum. Methods* **123**, 73 (1975).
- [9] S. E. Arnell, S. Sjöberg, Ö. Skeppstedt, E. Wallander, A. Nilsson, Z. P. Sawa, and G. Finnas, *Z. Phys. A* **289**, 89 (1978).
- [10] C. J. Lister, M. Campbell, A. A. Chishti, W. Galletly, L. Goettig, R. Moscrop, B. J. Varley, A. N. James, T. Morrison, H. G. Price, J. Simpson, K. Connel, and O. Skeppstedt, *Phys. Rev. Lett.* **59**, 1270 (1987).
- [11] M. A. C. Hotchkis, J. L. Durell, J. B. Fitzgerald, A. S. Mowbray, W. R. Phillips, I. Ahmad, M. P. Carpenter, R. V. F. Janssens, T. L. Khoo, E. F. Moore, L. R. Morss, Ph. Benet, and D. Ye, *Phys. Rev. Lett.* **64**, 3123 (1990).
- [12] E. K. Warburton, C. J. Lister, J. W. Olness, P. E. Haustein, S. K. Saha, D. E. Alburger, J. A. Becker, R. A. Dewberry, and R. A. Naumann, *Phys. Rev. C* **31**, 1211 (1985).
- [13] P. Chowdhury, C. J. Lister, D. Vretemar, Ch. Winter, V. P. Janzen, H. R. Andrews, D. J. Blumenthal, B. Crowell, T. Drake, P. J. Ennis, A. Galindo-Uribarri, D. Horn, J. K. Johansson, A. Omar, S. Pilotte, D. Prévost, D. Radford, J. C. Waddington, and D. Ward, *Phys. Rev. Lett.* **67**, 2950 (1991).
- [14] J. E. Kitching, P. A. Batay-Csorba, C. A. Fields, R. A. Ristinen, and B. L. Smith, *Nucl. Phys.* **A302**, 159 (1978).
- [15] E. K. Warburton, J. W. Olness, C. J. Lister, J. A. Becker, and D. S. Bloom, *J. Phys. G* **12**, 1017 (1986).
- [16] E. K. Warburton, J. W. Olness, C. J. Lister, R. W. Zurmühle, and J. A. Becker, *Phys. Rev. C* **31**, 1184 (1985).
- [17] Ch. Winter, D. J. Blumenthal, P. Chowdhury, B. Crowell, P. J. Ennis, C. J. Lister, C. J. Gross, J. Heese, A. Jungclaus, K. P. Lieb, J. Eberth, and S. Skoda, *Phys. Lett. B* **258**, 289 (1991).
- [18] M. Weiszflog, K. P. Lieb, F. Cristancho, C. J. Gross, A. Jungclaus, D. Rudolph, H. Grawe, J. Heese, K.-H. Maier, R. Schubart, J. Eberth, and S. Skoda, *Z. Phys. A* **342**, 257 (1992).
- [19] M. K. Kabadiyski, F. Cristancho, C. J. Gross, A. Jungclaus, K. P. Lieb, D. Rudolph, H. Grawe, J. Heese, K.-H. Maier, J. Eberth, S. Skoda, W.-T. Chou, and E. K. Warburton, *Z. Phys. A* **343**, 165 (1992).
- [20] S. E. Arnell, S. Sjöberg, Ö. Skeppstedt, E. Wallander, A. Nilsson, and G. Finnas, *Nucl. Phys.* **A280**, 72 (1977).
- [21] D. Bucurescu, G. Constantinescu, M. Ivaşcu, N. V. Zamfir, and M. Avrigeanu, *J. Phys. G* **7**, 399 (1981).
- [22] E. Matthias, E. Recknagel, O. Hashimoto, S. Nagamiya, K. Nakai, T. Yamasaki, and Y. Yamasaki, *Nucl. Phys.* **A237**, 182 (1975).
- [23] V. S. Shirley, in *Hyperfine Structure and Nuclear Radiations*, edited by E. Matthias and D. A. Shirley (North-Holland, Amsterdam, 1968), App. C.
- [24] O. Häusser, T. Faestermann, I. S. Towner, T. K. Alexander, H. R. Andrews, J. R. Beene, D. Horn, D. Ward, and C. Broude, *Hyperfine Interact.* **4**, 196 (1978).
- [25] F. W. N. de Boer, C. A. Fields, L. E. Samuelson, and J. Sau, *Nucl. Phys.* **A388**, 303 (1982).
- [26] K. Oxorn, S. K. Mark, J. E. Kitching, and S. S. M. Wong,



- Z. Phys. A **321**, 485 (1985).
- [27] H.-W. Müller and J. W. Tepel, Nucl. Data Sheets **54**, 527 (1988).
- [28] A. Nilsson and M. Grecescu, Nucl. Phys. **A212**, 448 (1973).
- [29] P. Kemnitz, J. Döring, L. Funke, G. Winter, L. H. Hildingsson, D. Jerrestam, A. Johnson, and Th. Lindblad, Nucl. Phys. **A456**, 89 (1986).
- [30] L. Funke, J. Döring, P. Kemnitz, E. Will, G. Winter, A. Johnson, L. Hildingsson, and Th. Lindblad, Nucl. Phys. **A455**, 206 (1986).
- [31] F. Dönau and S. Frauendorf, in *Proceedings of the Conference on High Angular Momentum Properties of Nuclei*, Oak Ridge, Tennessee, 1982, edited by N. R. Johnson (Hardwood Academic, New York, 1983), p. 143.